Journal of Experimental Botany, Vol. 63, No. 5, pp. 2203–2215, 2012
doi:10.1093/jxb/err427 Advance Access publication 5 January, 2012
This paper is available online free of all access charges (see http://jxb.oxfordjournals.org/open_access.html for further details)

Journal of Experimental Botany
www.jxb.oxfordjournals.org

RESEARCH PAPER

Physiological and proteomic approaches to evaluate the role of sterol binding in elicitin-induced resistance

Ladislav Dokládal[1], Michal Obořil[1], Karel Stejskal[3], Zbyněk Zdráhal[3], Nikola Ptáčková[1], Radka Chaloupková[2], Jiří Damborský[2], Tomáš Kašparovský[1], Sylvain Jeandroz[4], Markéta Žďárská[3] and Jan Lochman[1,*]

[1] Department of Biochemistry, Faculty of Science, Masaryk University, Kotlářská 2, 61137 Brno, Czech Republic
[2] Loschmidt Laboratories, Department of Experimental Biology and Research Centre for Toxic Substances in the Environment, Faculty of Science, Masaryk University, Kotlářská 2, 61137 Brno, Czech Republic
[3] Core Facility–Proteomics, Central European Institute of Technology (CEITEC), Masaryk University, Kamenice 5, 62500 Brno, Czech Republic
[4] UMR AgroSup Dijon/CNRS/INRA/Université Bourgogne ''Agroécologie'', 17 rue Sully, BP 86510, F-21065 Dijon cedex, France

* To whom correspondence should be addressed. E-mail: lochik@mail.muni.cz

Received 9 September 2011; Revised 28 November 2011; Accepted 30 November 2011

Abstract

Cryptogein is a proteinaceous elicitor secreted by *Phytophthora cryptogea* that can induce resistance to *P. parasitica* in tobacco plants. On the basis of previous computer modelling experiments, by site-directed mutagenesis a series of cryptogein variants was prepared with altered abilities to bind sterols, phospholipids or both. The sterol binding and phospholipid transfer activities corresponded well with the previously reported structural data. Induction of the synthesis of reactive oxygen species (ROS) in tobacco cells in suspension and proteomic analysis of intercellular fluid changes in tobacco leaves triggered by these mutant proteins were not proportional to their ability to bind or transfer sterols and phospholipids. However, changes in the intercellular proteome corresponded to transcription levels of defence genes and resistance to *P. parasitica* and structure-prediction of mutants did not reveal any significant changes in protein structure. These results suggest, contrary to previous proposals, that the sterol-binding ability of cryptogein and its mutants, and the associated conformational change in the ω-loop, might not be principal factors in either ROS production or resistance induction. Nevertheless, the results support the importance of the ω-loop for the interaction of the protein with the high affinity binding site on the plasma membrane.

Key words: Elicitins, intercellular proteome, ω-loop conformation, sterol binding, resistance induction.

Introduction

A successful plant defence is based on the early recognition of plant pathogens and fast activation of inducible defence responses. For this reason, pathogens have evolved strategies to avoid recognition by plants or to suppress its consequences. Pathogens usually secrete effector molecules (virulence factors) or even transfer them into the host cell to manipulate host physiology in their favour (Jones and Dangl, 2006). However, these effector molecules can be recognized via the products of plant resistance (*R*) genes and serve as avirulence (*Avr*) determinants for the host, mediating effector-triggered immunity (Luderer *et al.*, 2001; Jones and Dangl, 2006). This process has been described as a gene-for-gene relationship in which a plant *R* gene interacts with complementary *Avr* genes to cause disease resistance (Flor, 1971). The current conception suggests that products of *Avr* genes (elicitors) interact with specific plant-virulence targets, thereby inducing conformational changes that are detected by the plant R proteins (Jones and Dangl,

Abbreviations: DHE, 7-dehydroergosterol; LTPs, lipid transfer proteins; NBD-PC, nitrobenzoxadiazole-labelled phosphatidylcholine; PMSF, phenylmethanesulphonyl fluoride, ROS, reactive oxygen species; SAR, systemic acquired resistance.

2006; Wulff *et al.*, 2009). Consequently, a signalling process leading to plant defence is initiated.

Many pathogen Avr factors have been detected through their activity as elicitors of plant defence reactions; which are usually manifested as a hypersensitive response: a form of programmed cell death limiting the progression of pathogen attack. Several plant–pathogen models have been studied in detail and one of the experimentally accessible ones involves the interaction between tobacco and *Phytophthora*, a group of widespread and highly phytopathogenic oomycetes (for a review, see Ponchet *et al.*, 1999). Proteinaceous elicitors secreted by several *Phytophthora* and *Pythium* spp. are known under the term elicitins and are, in general, structurally similar to lipid-transfer proteins of plant cells (Ricci *et al.*, 1997; Blein *et al.*, 2002). They behave like sterol carrier proteins (Mikes *et al.*, 1998; Vauthrin *et al.*, 1999).

Cryptogein is a very efficient basic elicitin from *Phytophthora cryptogea*. The three-dimensional structure of cryptogein is composed of five α-helices, one β-sheet, and one ω-loop arranged in a unique protein fold (Boissy *et al.*, 1996; Gooley *et al.*, 1998). The ω-loop present in the structure of cryptogein is very flexible and highly conserved, which suggests it has an important function. The X-ray crystal structure of the cryptogein–ergosterol complex has a small conformational change in the ω-loop region, induced by binding of the sterol (Boissy *et al.*, 1999). Moreover, the recently determined structure of the β-cinnamomin–ergosterol complex has an almost identical structure to that of the cryptogein–ergosterol complex (Rodrigues *et al.*, 2006). Cryptogein binding studies and cross-linking experiments performed on tobacco plasma membrane resulted in the characterization of a single, low-abundance class of binding site with a K_d value of 2 nM, characterized as a glycosylated heterodimer protein (Wendehenne *et al.*, 1995; Bourque *et al.*, 1999). The perception step is followed by activation of protein kinases (PK) or inhibition of protein phosphatases (PP), triggering the Ca^{2+} influx which, in turn, triggers ROS production, MAPK activation, anion effluxes, and plasma-membrane depolarization as well as glucose (Glc) import inhibition or may lead to H^+-ATPase inhibition (for a review, see Garcia-Brugger *et al.*, 2006). Osman *et al.* (2001) assumed, on the basis of results with cryptogein mutants, under the sterol-binding hypothesis, that conformational changes in the ω-loop 'activate' elicitins, allowing them to bind effectively to high-affinity binding sites. On the other hand, Lochman *et al.* (2005) suggested that the conformational change of the ω-loop may be necessary to trigger early defence responses, such as the synthesis of reactive oxygen species (ROS), but not for the activation of later responses such as PR-protein expression and cell necrosis. However, since the mutations considered in that study were targeted to the ω-loop region they not only affected the sterol- and phospholipid-binding properties of cryptogein, but also slightly modified both the ω-loop structure and the overall protein structure.

The main goal of this study was to support or contradict the role of the elicitin–sterol complex in the induction of defence responses triggered by cryptogein. Site-directed mutagenesis of the elicitin cryptogein was performed in order to modify the residues that have been proposed to be responsible for sterol- and/or phospholipid-binding without modifying the ω-loop or overall protein structure. The ability of the mutants to bind sterols and/or to exchange phospholipids was investigated using fluorescence spectrometry along with characterization of the interaction of the mutants with the elicitin's putative receptor. The influence of the mutations on the course of the defence reaction in tobacco leaves was determined with respect to: (i) overall changes in the intercellular fluid proteome, and (ii) activation of resistance to the pathogen *P. parasitica*.

Materials and methods

Chemicals

Sterols and phospholipids, except nitrobenzoxadiazole-labelled phosphatidylcholine (NBD-PC) were purchased from Sigma and were dissolved in ethanol and chloroform (1 mg ml^{-1}), respectively. NBD-PC was purchased from Invitrogen and was dissolved in chloroform (5 mg ml^{-1}). Proteins were dissolved in water (1 mg ml^{-1}) and stored at –20 °C.

Plant material

Tobacco seeds (*N. tabacum* L. cv. *Xanthi*) were sown into peat soil, and plants were grown in controlled conditions (22 °C, 16 h light, 6000 lux, 80% r.h.). The experiments were done with 8-week-old plants.

Resistance analysis

Systemic acquired resistance (SAR) was induced by elicitin application (Ponchet *et al.*, 1999): plants were decapitated and their stems treated with 20 µl of water or a 5 µM aqueous solution of cryptogein. Inoculations with *P. parasitica* were performed by infiltrating leaf parenchyma tissue with a 50 µl suspension containing 100 zoospores (Hugot *et al.*, 1999). In each experiment, at least four consecutive leaves received two infiltrations of zoospore suspension each. Susceptibility and resistance were evaluated by measuring the areas over which disease symptoms were observed, at various numbers of days after inoculation, for each leaf since the development of disease symptoms is strictly correlated with the development of the oomycete (Galiana *et al.*, 1997). All experiments were performed at least three times with three replicates of plants. Results are presented as mean ±standard deviation. A Student's *t* test was used to analyse differences between two groups.

Isolation of recombinant proteins

The wild type (wt) cryptogein was expressed using the vector pPIC9 containing the X24 gene from *P.cryptogea* (isolate 52) with the addition of a Gly residue at the N-terminus to promote efficient post-transcriptional processing (namely α-secretion factor cleavage by the KEX2 protease). Site-directed mutagenesis was conducted using a QuikChange kit (Stratagene, France) and a pair of specific forward-reverse oligonucleotides (Metabion, Germany) to introduce the mutation to the targeted codon. The primers used for mutagenesis are given in Supplementary Table S2 at *JXB* online. The product was confirmed to have the expected DNA sequence, then the vector was used to transform *Pichia pastoris* and expression of the protein was induced in a Biostat B-DCU (Sartorius, Germany) fermentor using previously described protocol (Wood and Komives, 1999), with a methanol induction

phase of 48 h. The expressed protein was purified by ultrafiltration and Fast Protein Liquid Chromatography using a Source S15 column as described before (Pleskova *et al.*, 2011).

Fluorescence spectrometry

Fluorescence spectrometry was performed on a Perkin Elmer Luminescence Spectrometer LS 50B in a stirred cuvette. The sterol and phospholipid binding of proteins was measured according to previously described methods (Mikes *et al.*, 1997; Avdulov *et al.*, 1999) by the titration of proteins with DHE and NBD-PC in 10 mM MES buffer (pH 7.0). The excitation and emission wavelengths were 325 nm and 370 nm for DHE and 460 nm and 534 nm for NBD-PC. The values were read after equilibration. Dissociation constants, K_d, of the lipid–protein complexes were calculated as described in Lochman *et al.* (2005).

Sterol and phospholipid exchange assay

Elicitin-induced sterol exchanges were measured using stigmasterol or cholesterol micelles (3 μM) added to 2 ml measuring buffer (10 mM MES pH 7.0), containing DHE micelles (0.63 μM) (Vauthrin *et al.*, 1999). DHE fluorescence was then recorded in both the absence (to determine spontaneous transfer rates) and presence of the elicitins.

Elicitin-induced phospholipid exchanges were measured using NBD-labelled phosphatidylcholine (NBD-PC). Unilamellar donor vesicles containing NBD-PC, phosphatidylserine (PS) and cholesterol and acceptor vesicles (containing PC, PS, and cholesterol) were prepared as described previously (Pleskova *et al.*, 2011). Elicitin-induced phosphatidylcholine exchanges were measured by adding NBD-PC/PS (with 1.5 μM NBD-PC) donor vesicles to 2 ml measuring buffer (10 mM MES pH 7.0), containing PC/PS (with 3 μM PC) unilamellar acceptor vesicles, then recording the fluorescence of NBD-PC in both the absence (to determine spontaneous transfer rates) and presence of the elicitins.

Measurement of reactive oxygen species

ROS production was determined by chemiluminescence. Twenty minutes after the addition of elicitins to the tobacco cell suspensions, aliquots of 250 μl were collected from the batch of treated cell suspensions and mixed with 300 ml of 10 mM HEPES buffer, pH 6.5, 175 mM mannitol, 0.5 mM $CaCl_2$, 0.5 mM K_2SO_4, and 50 ml of 0.3 mM luminol (Poinssot *et al.*, 2003). Chemiluminescence was monitored every 10 min with a Lumat LB 9507(Berthold) luminometer (signal integrating time of 10 s).

Tobacco intercellular fluid isolation

Upper, middle, and lower leaves, each from a different tobacco plant (from five plants in total), were cut off and immersed in 250 nM cryptogein solutions. After 48 h the leaves were rinsed in water to remove any debris from the surfaces and any cytoplasmic contaminants from the cut edges, then vacuum-infiltrated for 5 min at room temperature with an isolation buffer containing 25 mM TRISs-Cl pH 7.8, 10 mM $CaCl_2$, 5 mM 2-mercaptoethanol, and 1 mM PMSF. The plant material was then blotted and rolled into the barrel of a 20 ml plastic syringe, which was subsequently placed, hub down, in a 50 ml centrifuge tube and centrifuged at 800 *g* for 10 min at 4 °C. The tobacco intercellular fluid isolates collected at the bottom of the tubes were stored at –20°C. The tobacco leaves were stored at –80 °C for later use in chlorogenic acid, capsidiol, and real-time PCR analyses.

Proteomic analysis

The tobacco intercellular fluid isolates were concentrated using ultrafiltration devices (Vivaspin 6 Concentrator, GE Healthcare, USA) with a 3 kDa cut-off by centrifugation at 8000 *g* at 4 °C, then rediluted in a sample buffer containing 8 M urea, 2% (w/v) CHAPS, 65 mM DTT, and 2% (v/v) IPG buffer (carrier ampholyte mixture, GE Healthcare, USA) and reconcentrated using the same procedure. Finally, the samples were diluted 10-fold with the sample buffer. The total protein concentration was determined with an *RC DC* Protein Assay Kit (Bio-Rad, USA) using a calibration curve for BSA. For isoelectric focusing, Immobiline DryStrip pH 3–11 NL, 7 cm (GE Healthcare, USA) were used. Passive sample application during rehydration was performed. In each case, 80 μg of total protein in the sample buffer was loaded in triplicate. The rehydration time was 18 h. The IEF was performed using a PROTEAN IEF Cell (Bio-Rad, USA). See the Supplementary data at *JXB* online for detailed conditions of focusing and SDS-PAGE analysis. Owing to the low overall concentration of the proteins isolated from the intercellular fluid, gel-staining using a highly sensitive fluorescent stain, SYPRO Ruby (Bio-Rad, USA), was used. The gels were then rinsed in the fixing solution for 60 min and subsequently washed in water before imaging with a Pharos FX Plus Molecular Imager (Bio-Rad, USA). The gels were further analysed using PDQuest software (Bio-Rad, USA) and selected spots were identified by MS analysis.

Mass spectrometric analysis

Protein spots selected for analysis were excised from 2-DE gels with an EXQuest Spot Cutter (Bio-Rad, USA). After destaining, the proteins in the gel pieces were incubated with trypsin (sequencing grade, Promega, USA) at 37 °C for 2 h. The corresponding proteolytic digests were analysed with MALDI-MS/MS and LC-MS/MS.

MALDI-MS and MS/MS analyses were performed on an Ultraflex III mass spectrometer (Bruker Daltonik, Germany) using a CHCA matrix in combination with an AnchorChip target. LC-MS/MS analysis was performed online using an EASY-nLC system (Proxeon) coupled with an HCTultra PTM Discovery System ion trap mass spectrometer equipped with a nanospray (Bruker Daltonik, Germany). LC separation was accomplished on a reverse-phase column with a water/acetonitrile gradient. The MASCOT 2.2 (MatrixScience, London, UK) search engine was used for processing the MS and MS/MS data. Database searches were done against the NCBI protein database and EMBL EST plant database. See Supplementary Data for detailed conditions of mass spectrometric analyses.

Transcription levels of defence genes

The expression of genes in leaf tissues was analysed by real-time quantitative PCR (RT-qPCR), using the fluorescent intercalating dye SYBR-Green, in a Light Cycler 480 (Roche). Total RNA was isolated from 100 mg of leaf tissue using TRI reagent (Ambion, USA) and purified using the TURBO DNA-free kit (Ambion, USA). Reverse transcriptase reactions were performed with the ImProm-II Reverse Transcription System (Promega, USA), with 0.4 μg of total RNA in a volume of 20 μl, according to the manufacturer's instructions. cDNA was amplified by qPCR using gene-specific primers (see the Supplementary data and Supplementary Table S2 at *JXB* online) and GoTaq qPCR Master Mix (Promega, USA) according to the manufacturer's instructions. PCR amplification was carried out as follows: 45 cycles of DNA denaturation at 95 °C for 20 s, annealing and extension at 60 °C for 40 s, with three replicates for each analysed sample. The transcript level of each gene was normalized to that of elongation factor 1α (EF-1α) to facilitate the quantification of gene expression relative to an endogenous control by the $\Delta\Delta C_T$ method. It was shown previously that the expression of elongation factor 1α is not influenced by different stress conditions (Nicot *et al.*, 2005).

Preparation of plasma membrane

Tobacco cell suspensions (*Xanthi*) were cultivated in Chandler medium on a rotary shaker (150 rpm, 25 °C) under continuous

light (photon flux rate 30–40 μmol m^{-2} s^{-1}). Cells were maintained in the exponential phase. Plasma membrane-enriched fractions were obtained following the aqueous partitioning procedure as described previously (Svozilova *et al.*, 2009).

Right orientation of isolated plasma membranes was verified by measurement of ATPase activity when total ATPase activity was obtained in the presence of 0.01% Triton X-100, while the latent activity was given by the difference between the activities in the presence and absence of Triton (Svozilova *et al.*, 2009).

Quantification of receptor sites on plasma membranes

Cryptogein and its mutants were fluorescently labelled with fluorescein isothiocyanate as described previously (Hermanson, 1996). Binding experiments were performed as described previously (Osman *et al.*, 2001) when plasma membrane preparations containing 50 μg of protein were used and non-specific binding was determined in the presence of 10 μM unlabelled proteins. The bound ligand was separated by filtration through the GF/B filter (Whatman) pre-soaked in 1% BSA (Osman *et al.*, 2001). Finally, fluorescently labelled proteins were released from the surface of the filter using 0.1% SDS (15 min incubation at 4 °C) and fluorescence was measured using a fluorimeter (Horiba Yvone, France) (Svozilova *et al.*, 2009). The content of the receptor was calculated using known standard amounts of the protein–FITC conjugate placed on the filters. The calibration curve in the range from 5 ng.ml^{-1} to 1 μg ml^{-1} was linear up to 1 μg of proteins. The number of binding sites was calculated using the known molecular masses of proteins.

Chlorogenic acid analysis

Chlorogenic acid was analysed in both intercellular fluid isolates and leaf extracts. Intercellular fluid isolates were prepared as described above. Leaf extracts were prepared from 150 mg of plant tissue, which was added to 1 ml of 33% (v/v) acetone in water and disintegrated in a grinding mortar with sea sand. The contents of the mortar were then pipetted into a microtube and extraction was carried out with ultrasound treatment (100 W, 15 min). After centrifugation (10 min, 13 000 *g*), 50 μl of sample was analysed by high-performance liquid chromatography (HPLC) using an HP 1100 HPLC system (Agilent, Germany), equipped with a DAD detector set at 210 nm, an LC-8-DB (25 cm×4.6 mm I.D.) reverse-phase column (Supelco) with solvent A [0.25% (v/v) H_3PO_4 in water] and solvent B (acetonitrile). The elution gradient was as follows: 0-5 min, 0-5% of B; 5-15 min, 5-15% of B; 15-20 min, 15-20% of B; 20-21 min, 20-60% of B. The flow rate was 1 ml min^{-1} and the column temperature was 24 °C. The signal was monitored at 254 nm and 320 nm. For quantification purposes a calibration curve was made.

Capsidiol analysis

150 mg samples of leaves collected 48 h after application were ground with 500 μl of 90% methanol. Then, 50 μl portions of the resulting extracts were centrifuged (12 000 *g*, 10 min) then analysed by HPLC following the method described by Literakova *et al.* (2010), using an HP 1100 HPLC system (Agilent, Germany), equipped with a DAD detector set at 210 nm, an LC-8-DB (4.6 mm I.D.×25 cm) reverse-phase column (Supelco) as the stationary phase and an aqueous methanol gradient as the mobile phase.

Results

Dobeš and co-workers used computer modelling and quantitative structure–activity relationship analysis to design cryptogein variants with altered binding of lipid compounds (Dobeš *et al.*, 2004). Construction and biochemical characterization of these mutants should provide an insight into the role of lipid binding over the course of a defence reaction. Three recombinant cryptogeins carrying the following mutations were prepared: Leu41Phe, Val84Phe, and both Leu41Phe and Val84Phe. The mutated residues targeted a hydrophobic cavity of the elicitins. The proteins were produced using the eukaryotic *P. pastoris* expression system, to ensure that they retained their native folded structures. Molecular weights (MW) of the proteins were determined by MALDI MS: 10 386 Da for cryptogein, 10 418 Da for the Leu41Phe mutant, 10 433 Da for the Val84Phe mutant, and 10 467 Da for the Leu41Phe/Val84Phe double mutant. The measured values were in good agreement with the calculated values. The observed mass difference between measured and theoretical MWs (6 Da) corresponded to three disulphide bridges. The proteins overall structure was confirmed by circular dichroism (CD) spectroscopy (Fig. 1). The CD spectra confirmed that their secondary structure, which is *c.* 50% α-helix with little β-structure, is largely conserved, as previously shown (Gooley *et al.*, 1998). The mutations slightly modify a number of amino acids in the α-helical region.

Sterol-binding activities and affinities

Elicitins have a hydrophobic core that can accommodate sterols or phospholipids. The sterol-binding activity of the wt cryptogein and the Leu41Phe, Val84Phe, and Leu41Phe/Val84Phe mutants was determined using the fluorescent sterol dehydroergosterol (DHE). To exclude possible effects of non-specific binding, aprotinin was included as a negative control in all binding experiments since it has very similar properties to cryptogein (MW=6.5 kDa, p*I*=10.1). Addition of aprotinin did not affect the DHE fluorescence in the assays. The binding parameters of sterol to the proteins (K_d) were calculated from the fluorescence data (Table 1) and corresponds to previous published data (Mikes *et al.*, 1997,

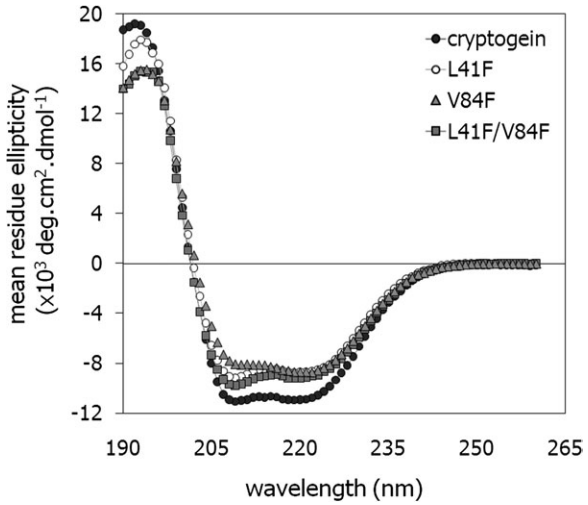

Fig. 1. Analysis of secondary structures of elicitins. Far-UV circular dichroism spectra of wt cryptogein (filled circles), the V84F mutant (filled triangles), the L41F mutant (open circles), and the L41F/V84F double mutant (filled squares). Protein concentration: 0.2 mg ml^{-1}, solvent: water, light path: 0.1 cm, room temperature.

Table 1. DHE binding and lipid transfer activities of studied proteins

Dissociation constants, K_d, of analysed proteins for DHE binding and initial rates of sterol (DHE) and phospholipid (PC) transfer measured by changes in DHE and NBD-PC fluorescence. Fluorescence curves used for calculations are shown in Supplementary Fig. S1 at *JXB* online.

Protein	K_d (μM)	DHE transfer	NBD-PC transfer
Cryptogein wt	0.56±0.04	2.51±0.06	0.51±0.05
L41F	0.85±0.05	1.88±0.08	0.32±0.01
V84F	No binding	0.45±0.02	0.74±0.08
L41F/V84F	No binding	0.38±0.01	0.76±0.04
Aprotinin	No binding	0.19±0.01	0.15±0.01

1998; Hirasawa *et al.*, 2004). For all measured proteins the number of binding sites was found to be approximately one per molecule.

Sterol and phospholipid transfer

From a physiological point of view, an important feature of elicitins is their ability to interact with the plasma membrane and transfer sterols and phospholipids. To evaluate the ability of the elicitins to transfer sterols, the initial rates of fluorescence increase after the addition of elicitins to micelles was determined. Previously, it was shown that the micelle method gave comparable results with that using fluorescence polarization in phospholipid vesicles (Vauthrin *et al.*, 1999). The addition of wt cryptogein stimulated a rapid increase in fluorescence with a plateau after about 5 min owing to dilution of DHE in the stigmasterol micelles. The initial rates of fluorescence for wt cryptogein and the mutants are given in Table 1. As expected, cryptogeins containing the Val84Phe mutation showed a significantly reduced ability to transfer DHE between the membranes compared with wt cryptogein. In the case of the Leu41Phe mutant, only a minor decrease in DHE transfer rate was observed. It could be argued that cryptogeins containing Val84Phe mutation bind sterols as well but their loading rates might be too small to be detected by the fluorescence method used which could explain the apparent inconsistency in the results of the sterol-binding assay.

The transfer of phospholipids between the membranes was evaluated using a method based on the exchange of the fluorescently labelled phospholipid NBD-PC (nitrobenzoxadiazole-labelled phosphatidylcholine) from unilamellar donor vesicles to PC (phosphatidylcholine) acceptor vesicles as described in the Materials and methods. Individual rates of fluorescence after addition of the elicitins are given in Table 1. Surprisingly, the Val84Phe mutant and the double mutant showed higher rates of PC transfer than did cryptogein. On the other hand, and consistent with expectations, the Leu41Phe mutant showed a lower rate of PC transfer. Similarly to the sterol-binding experiments, aprotinin was used as a control to exclude the possibility of non-specific transport by the elicitins. It did not elicit transport of sterols or phospholipids between the membranes (Table 1).

Induction of early events by mutated cryptogeins in tobacco cells in suspension

The effects of the mutations on the elicitation of the synthesis of ROS in tobacco cells in suspension were measured. Suspension cultures enable the exact parallel evaluation of the early events over time. The tobacco cell suspensions were elicited with 10 nM cryptogein solutions. The levels of hydrogen peroxide over time are shown in Fig. 2B. The double mutant Leu41Phe/Val84Phe stimulated almost no synthesis of ROS. On the other hand, although the Val84Phe mutant was unable to bind DHE (Table 1), it was almost as efficient as the wt cryptogein in stimulating ROS synthesis. The production of ROS stimulated by the Leu41Phe mutant, which showed a lower ability to transfer PC, was about half that of wt cryptogein, with the maximum shifted to 10 min.

Proteomic analysis

To study the effect of the four cryptogeins on the expression of proteins involved in the defence response, an analysis of intercellular fluid (IF) was conducted. The main reason for analysis of IF was that acidic PR proteins are secreted into IF during the defence response (van Loon *et al.*, 2006). Tobacco leaves were treated by soaking the petioles in 250 nM aqueous solutions of the cryptogeins for 48 h. Varying levels of necrosis, up to one-third of the leaf area, were observed for the different proteins (Fig. 2A). The Leu41Phe mutant and the Leu41Phe/Val84Phe double mutant induced almost no necrotic symptoms and the Val84Phe mutant induced a lower extent of necrosis than wt cryptogein.

To minimize protein losses during sample preparation for IEF, the precipitation step was omitted. For a triple 2-D separation of one sample, isolates from 15 leaves were used, namely upper, middle, and lower leaves from each of five plants. Moreover, chlorogenic acid, an intracellular marker of plant cells, was analysed in both intercellular fluid isolates and leaf extracts to estimate the extent of intracellular contamination in intercellular fluid isolates. The calculated contaminations in all samples did not exceed 8%. A massive induction of protein expression into tobacco intercellular space after treatment of leaves with the elicitins was observed. The highest correspondence in counted spots was found for wt cryptogein and the Val84Phe mutant (65%) and, as expected, the lowest one was found for the control and wt cryptogein (6%). The sixty-five most intense spots that differed qualitatively between control and individual elicitins were excised from the two-dimensional gels and identified by tandem mass spectrometry (MALDI-MS/MS and LC-MSMS). Good spectra were obtained from 45 of the digests and it was possible to identify 34 of the spots unambiguously. Taking into account the multiplicity of spots, a total of 21 unique proteins were identified (Table 2; for details see the Supplementary data,

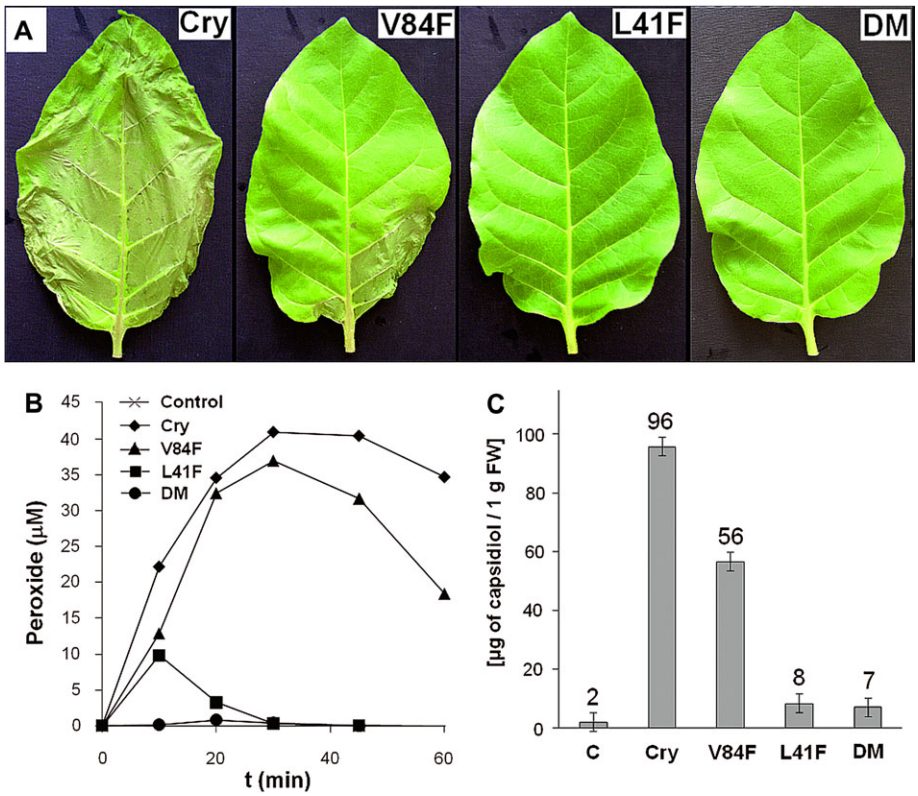

Fig. 2. Extent of leaf necrosis, AOS production, and capsidiol content after application of individual elicitins. (A) Leaves with the most extensive necrosis 3 d after treatment with 250 nM elicitins solutions. (B) ROS synthesis in tobacco cells in suspension stimulated by 10 nM elicitins: wt cryptogein (diamonds), V84F (filled triangles), L41F (squares), L41F/V84F (circles), and control (X). Cells were equilibrated for 3 h in an elicitation buffer, and elicitins were added to the suspension at the time zero. The concentrations of H_2O_2 were monitored every 10 min in 250 μl aliquots by a luminol method. (C) Capsidiol content analysed by HPLC analysis 2 d after treatment with 250 nM elicitins solutions, results for three independent analyses of each sample were averaged. Cry, wt cryptogein, DM, L41F/V84F double mutant.

Supplementary Table S1, and Supplementary Fig. S2 at *JXB* online). The majority of the identified proteins play a role in plant–pathogen interactions and are naturally located extracellularly.

Surprisingly, the results do not show a strong correlation between the ability of an elicitin to bind or transfer sterols or phospholipids and the expression of extracellular proteins with defence response roles. Similarly, although the Leu41Phe mutation does not significantly alter the sterol transfer rates, it has a strong influence on the expression of defence proteins. The potential role of the identified proteins in plant–pathogen interaction and the dependence of their expression on elicitin design are further described in the Discussion.

Accumulation of defence gene transcripts

To investigate the relationship between the proteomic data and gene expression, the transcript levels for selected proteins were evaluated with RT-qPCR assays. Based on the results of proteomic analysis, the following genes were selected for transcript quantification: *PR2Q*, *PR3Q*, *PR5*, *GLN2*, *TuReP*, *NtPRp27*, and *GeLiP*. Transcript levels of all of these determined genes were related to those induced in the water sample used as a control. The results are summarized in Table 3 showing correlations with the proteomic data. For the double mutant, no or only a minimal increase in transcript levels was observed whereas for the Val84Phe mutant the increases in transcript levels were similar to or higher than those observed for cryptogein.

Accumulation of capsidiol

Capsidiol production is triggered either by pathogen attack or by biotic and abiotic elicitors; it acts as an anti-microbial compound against pathogens (Facchini and Chappell, 1992). From tobacco leaves, extracts for a reverse-phase HPLC-based capsidiol analysis were prepared as described in the Materials and methods. The results of the analysis are shown in Fig. 2C. The Leu41Phe mutant and Leu41Phe/Val84Phe double mutant showed a very low ability to trigger capsidiol synthesis, which correlates well with reductions in their ROS accumulation and necrotic effects.

Resistance to P. parasitica

The results presented above, particularly from the proteomic analysis, suggest that introduction of the Leu41Phe mutation to cryptogein would reduce the level of resistance

Table 2. Identified proteins whose expression qualitatively differed after treatment with cryptogein and its mutants
List of differentially expressed proteins identified by MALDI-MS/MS and/or LC-MS/MS including their individual spot numbers and presence (+). The corresponding NCBI accession numbers, the theoretical molecular weight (MW), and p*I* values are also indicated. The Mascot scores and protein coverage (%) for all identified proteins are listed in Supplementary Table S1 at *JXB* online.

Protein	NCBI accession no.	Spot no.	MW (kDa)	p*I*	Cry[a]	L41F	L41F/V84F	V84F
β−1,3−glucanases								
Glucan endo-1,3-β-glucosidase	19859	4	37.8	5.2	+			+
Glucan endo-1,3-β-glucosidase	19869	13, 14, 15	40.4	7.1	+			+
Chitinases								
CBP20	632736	8, 12, 17	21.9	8.4	+	+	+	+
PR-4A	19962	8	16.2	7.6	+		+	+
PR-4B	100352	19, 21	15.2	6.1	+	+	+	+
Endochitinase A	116314	14, 15	35.1	8.4	+			+
Endochitinase B	116321	16	34.7	8.3	+			+
Acidic chitinase PR-P	19771	22, 24	27.5	4.9	+	+		+
Acidic chitinase PR-Q	19773	3, 18	27.6	5.1	+	+		+
NtChitIV chitinase	121663827	23, 5	29.9	4.9	+			+
Chi-5 (Chitinase/lysozyme)	467689	12	42.0	9.1	+			+
Proteinase inhibitors								
Proteinase inhibitor I-A	547732	9	11.9	7.8	+			+
Proteinase inhibitor I-B	547733	9	11.9	7.8	+			+
Peroxidases								
Lignin-forming anionic peroxidase	129837	1, 2, 20, 21	34.7	4.7	+	+	+	+
Peroxidase	63002585	15	35.6	8.4	+			+
Peptidyl-prolyl isomerases								
Cyclophilin-like protein	152206078	11	22.0	7.8	+			+
Peptidyl-prolyl isomerase, putative [*Ricinus communis*]	255547634	10, 11	27.5	9.6	+			+
Other								
Germin-like protein	222051768	6	21.4	5.8	+		+	+
NtPRp27	5360263	25	27.4	9.3	+			+
Thaumatin-like protein E22	131015	22	24.7	5.4	+	+		+
Tumour-related protein	1762933	7	23.4	8.5	+			+

[a] Cry, wt cryptogein.

Table 3. Accumulation of defence-related genes

Effect of wt cryptogein and the mutants L41F, L41F/V84F, and V84F on accumulation of transcripts for PR and other defence-related proteins. Gene expression relative to a control was calculated by the $\Delta\Delta C_T$ method. The values given in the table are the logarithm of the relative increase (logR) and its standard deviation (SD). More than a 2-fold increase in gene expression was taken as significant.

Gene	A.N.[a]	Cry[b] logR	SD	V84F logR	SD	L41F logR	SD	L41F/V84F logR	SD
PR2Q									
β−1,3−glucanase	X54456	1.04	0.12	1.32	0.12	0.80	0.09	0.03	0.12
GLN2									
β−1,3−glucanase	X53600	1.08	0.13	1.12	0.13	0.64	0.14	−0.10	0.12
PR3Q									
Chitinase	X51425	1.02	0.15	1.00	0.11	0.57	0.12	−0.07	0.10
PR5									
Thaumatin-like protein	X12739	1.23	0.19	1.76	0.11	1.04	0.07	0.35	0.10
TuReP									
Tumour-related protein	FG644925	2.35	0.13	1.83	0.04	0.68	0.15	0.28	0.07
NtPRp27	FG633857	1.02	0.15	1.29	0.12	0.67	0.07	0.51	0.06
GeLiP									
Germin-like protein	AB449366	0.64	0.13	0.82	0.05	n.d.	n.d.	0.46	0.11

[a] A.N., accession number of gene in NCBI database. [b] Cry, wt cryptogein.

induced. To verify this, resistance of tobacco plants to the oomycete *P. parasitica* was evaluated. As expected, there was no induction of resistance for plants treated with the Leu41Phe mutant or the Leu41Phe/Val84Phe double mutant. The resistance induced by the Val84Phe mutant was comparable with that of wt cryptogein (Fig. 3).

Binding experiments

FITC-labelled elicitins were used to measure the affinity of the different mutants to specific binding site on the plasma membrane. Specific binding of FITC-elicitins was determined at two different elicitins concentrations (10 nM and 30 nM) in which a significant difference was observed in the binding of cryptogein and its mutants with an altered ability to bind sterol as previously described by Osman *et al.* (2001). At 10 nM elicitins concentration, the amount of bound molecules was 57.4±4.8 and 55.3±8.4 pmol mg^{-1} plasma membrane proteins for cryptogein and the mutant Val84Phe, respectively. By contrast, the mutants Leu41Phe and Leu41Phe/Val84Phe exhibited almost no specific binding (Fig. 4). At 30 nM concentration, the amount of bound molecules for cryptogein and the mutant Val84Phe was similar to that at 10 nM concentration, while for the mutants Leu41Phe and Leu41Phe/Val84Phe increased to 14.4±1.4 and 16.9±2.9 pmol mg^{-1} plasma membrane proteins, respectively (Fig. 4). The results obtained showed noticeable difference in the binding behaviour of elicitins and correspond well with other measured parameters of studied elicitins.

Discussion

In tobacco plants, elicitins induce a hypersensitive response and non-specific SAR (Keller *et al.*, 1996). The most efficient elicitin is cryptogein (from *P. cryptogea*), the less efficient ones being parasiticein and capsicein, secreted by *P. parasitica* and *P. capsici*, respectively (Ponchet *et al.*, 1999). Despite differences in the induction of defence responses, they share a similar high-affinity binding site located on the plasma membrane and have similar K_d (Buhot *et al.*, 2001). Moreover, it has been shown that wheat LTP1, which shows *in vitro* toxicity to a broad range of host and non-host fungal pathogens, interacts with this elicitin's receptor as well (Sun *et al.*, 2008). These opposing facts prompted the question as to how the elicitins are perceived by the plants. Previous studies (Osman *et al.*, 2001; Lochman *et al.*, 2005) assumed a role for sterol binding in determining the biological activity of elicitins. However, the conclusions drawn are not fully concordant and apparent discrepancies remain to be explained. In this study, an attempt was made to clarify the relationship between the lipid-loading properties of elicitins and the course of the defence reaction through the construction of three new cryptogein mutants, Leu41Phe, Val84Phe, and the double mutant Leu41Phe/Val84Phe. In contrast to the previous study of Lochman *et al.* (2005), in these mutants no structural changes due to the mutations were expected (Dobeš *et al.*, 2004).

Interaction of mutated cryptogeins with sterols and lipids

Previously, it has been shown that elicitins are able to bind and transfer sterols and phospholipids (through their fatty acid chains), for example, the SCP-2 protein from rat liver has similar binding and transfer properties for sterols and phospholipids (Mikes *et al.*, 1998; Pleskova *et al.*, 2011). Data from sterol (specifically, DHE) binding assays were in agreement with expectations based on the structural data of the DHE-cryptogein and fatty acid–cryptogein complexes

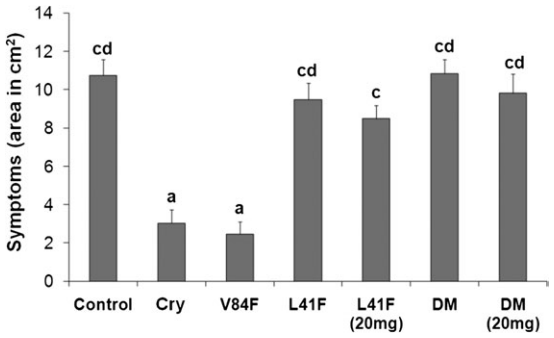

Fig. 3. Induction of resistance against *Phytophthora parasitica* in tobacco plants. Leaves from 8-week-old tobacco plants treated with elicitins were inoculated with zoospores of *P. parasitica*. The invaded areas were measured 3 d after inoculation. Each bar represents the standard error of four replicates from three different experiments. A replicate corresponds to eight inoculated areas on four leaves from one plant. Student's *t* test with P=0.01 was used to determine whether differences in area were statistically significant. Different letters represent significant difference. Cry, wt cryptogein.

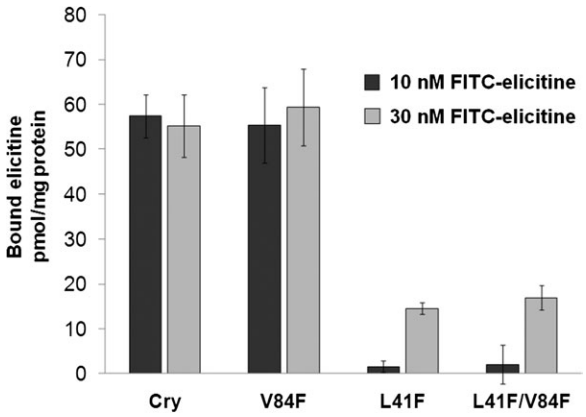

Fig. 4. Specific binding of the elicitins to the high-affinity sites located on tobacco plasma membranes. The number of binding sites was obtained with FITC-labelled elicitins. Plasma membrane preparations were incubated with 10 nM and 30 nM concentrations of labelled elicitins. The experiments were repeated three times and the results are expressed as the mean values ±SD (pmol bound elicitin/mg plasma membrane proteins).

reported previously (Dobeš *et al.*, 2004). Substitution of Val84 with phenylalanine reduced the binding and transfer rate of the sterol (DHE) between the micelles and the Leu41Phe mutation reduced the transfer rate of PC. The unexpectedly higher rate of PC exchange in mutants carrying the Val84Phe substitution can be explained by the fact that mutation of a small valine residue for a large phenylalanine residue could have resulted in a relaxing of the cavity groove, facilitating the binding of highly flexible fatty-acid chains of phospholipids.

Effect of mutations on the induction of early and late defence responses

Both previous studies (Osman *et al.*, 2001; Lochman *et al.*, 2005) focused on the contribution of sterol-binding to elicitin activity and suggested the necessity of a conformational change in the ω-loop (induced by sterol binding) to induce the early events (ROS production and pH changes). Contrary to this suggestion, the Val84Phe mutant, with a substantially lowered ability to bind and transfer sterols, was as efficient as wt cryptogein in stimulating ROS production with the same kinetics and intensity; and the Leu41Phe mutant, with only a slightly lowered ability to bind and transfer sterols, was far less efficient in inducing the synthesis of ROS (Fig. 2). Surprisingly, given these findings, the Leu41Phe/Val84Phe double mutant showed almost no ability to transfer and bind sterols, and led to almost no ROS synthesis. To clear up this discrepancy, the structures of mutants having the Leu41Phe mutation were elucidated. The CD spectra showed that the mutations only slightly modify a number of amino acids in the α-helical regions. Moreover, structure-prediction of the Leu41Phe and Leu41Phe/Val84Phe mutants was done according to three different methods and with two different software tools and revealed that the large phenylalanine(s) are easily accommodated by the surrounding residues without any significant changes in the ω-loop (Fig. 5). On the other hand, the Leu41Phe residue is highly conserved among elicitins and the binding experiment showed significantly reduced binding activity for mutants having Leu41Phe mutations (Fig. 4). These finding led to the hypothesis that the mutation of a small leucine residue for a large hydrophobic phenylalanine residue alters the interaction of the protein with the high-affinity binding site on the plasma membrane. To test this hypothesis, the double mutant Leu80Phe/Val84Phe was constructed and preliminary results supported the hypothesis, since the double mutant Leu80Phe/Val84Phe showed similar characteristics to the Val84Phe mutant (for details see the Supplementary data at *JXB* online). Detailed characterization of elicitin interaction with this high-affinity binding site is ongoing in our laboratory.

The analysis of intercellular proteome changes triggered by individual mutants revealed qualitative changes in proteins that play an important role in resistance processes (Table 2). In mutants having the Leu41Phe mutation, a strong reduction in such proteins was observed. These

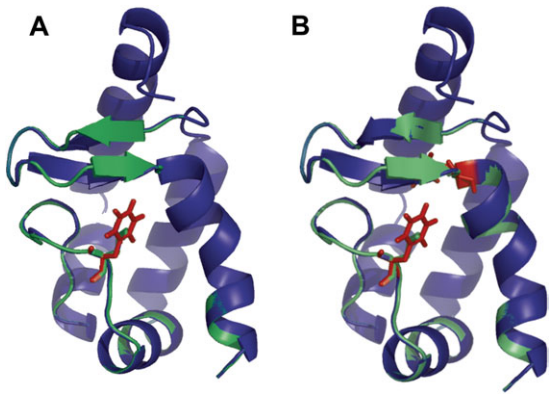

Fig. 5. Structural alignment of the wild-type (green) and the L41F mutant (A, blue), L41F/V84F mutant (B, blue) of the cryptogein prepared by Swiss-PdbViewer (Guex and Peitsch 1997). The side-chains of the mutated residues (red) adopt the conformation without disruption of omega loop or entire protein structure. The most obvious difference is the extension of one of the β-strands in the β-hairpin. The structural minimization with GROMOS force-field was conducted using 10 000 steps of steepest descent followed be several rounds of 10 000 steps of conjugate gradient. The picture was generated using PyMol (DeLano Scientific Ltd., USA).

proteins included two different β-1,3-glucanases (PR-2 family), which have been shown to suppress diseases caused by different pathogens (Grover and Gowthaman, 2003); proteinase inhibitors targeting nematodes and herbivorous insects (Casaretto and Corcuera, 1995); peptidyl-prolyl isomerases with antifungal and antiviral activities (Wong *et al.*, 2010); NtPRp27 protein, which accumulates after TMV infection and wounding (Okushima *et al.*, 2000); and tumour-related protein (Table 2). In addition, four chitinases belonging to the PR-3 family were identified only in the Val84Phe and wt cryptogein samples: endochitinases A and B, which inhibit the growth of many fungi *in vitro* (Rohini and Rao, 2001; Selabuurlage *et al.*, 1993); and chitinases belonging to class IV (NtChitIV) and class V (Chi-V) having an important function in early general defence responses (Shinya *et al.*, 2007) or synergistic antifungal activity with class I β-1,3-glucanase (Melchers *et al.*, 1994). The last protein identified only in Val84Phe and wt cryptogein samples was a peroxidase of molecular weight 35.6 kDa showing a very high homology to the gene *tpoxN1*, belonging to the class III of plant peroxidases induced by wounding (Hiraga *et al.*, 2000). The observed changes in the intercellular fluid proteome induced by cryptogein and the mutants were in concordance with the synthesis of ROS in cell suspension, the capsidiol level (acting as an antimicrobial compound) in extracellular fluid, and resistance to *P. parasitica*.

All these findings contradict the study of Osman *et al.* (2001). At first sight the inconsistency of the obtained data with those published by Lochman *et al.* (2005) which suggested the lack of any relationship between the ability of elicitins to induce the production of PR proteins, together with tissue necrosis and sterol-binding properties, is clear as well. But if the fact that residues Met35 and Leu36 in the

ω-loop are highly conserved among elicitins is taken into consideration, as in the case of the Leu41Phe mutant, their mutation to large bulky residues (tryptophan and phenylalanine) could have resulted in an altered interaction with the high-affinity binding site, which was not determined. Consequently, this effect could have been responsible for a longer lag phase (especially at the lower concentration) before the pH changes and ROS production, but it had minimal effect in the late phase of cell necrosis or the expression of defence genes.

The role of sterol binding in elicitin activity

The lack of correlation between binding and response of the different elicitins and LTPs cannot be easily explained. The three-dimensional structures of the basic elicitins cryptogein, cinnamomin, and LTP1 have been elucidated by crystallography (Gincel *et al.*, 1994; Boissy *et al.*, 1996; Rodrigues *et al.*, 2006). Moreover, the crystal structures of the free and sterol-bound forms of cryptogein and cinnamomin have been elucidated. In both structures, sterol binding induces a slight movement of the ω-loop and significant changes in residues Tyr87, Met35, and Leu15. A structural alignment of LTP1 with cryptogein revealed superimposition of the helices H_A, H_D, and H_E of cryptogein with the H_3, H_1, and H_2 helices of LTP1, suggesting a possible role of these elements in binding to a common high-affinity membrane binding site (Buhot *et al.*, 2001). From this point of view, the role of the ω-loop in binding to the receptor seems to be less important; but this does not rule out its role in the 'activation' of elicitins. However, the Leu41Phe mutation shows that some conserved amino acids in the ω-loop may play an important role in the binding process as well.

The full role of the change in the ω-loop structure induced by sterol binding is unclear. Osman *et al.* (2001) suggested the necessity of this change for elicitin activation but the results of Lochman *et al.* (2005) suggested that the ω-loop played a role only in the induction of the early events. A summary of the results of this study (Table 4) shows no relation between a cryptogein's sterol-binding activity and its defence-reaction induction, which contradicts both previous hypotheses. However, at the very least, the affinities and activities of the Tyr47Gly mutant observed by Osman *et al.* (2001) need to be interpreted with caution. The tyrosine residue 47 in helix C of cryptogein is involved in the sole hydrogen bond between the protein core and the sterol hydroxyl but is also strongly constrained because of the stacking of the phenol ring with the side chains of Pro42 and Tyr33 (Boissy *et al.*, 1999). Neither phenylalanine nor glycine is able to form a hydrogen bond with the sterol hydroxyl, hence a similar effect to that of sterol binding and hence similar protein activities should be expected according to the proposed working scheme of elicitin action. Nevertheless, high variances in individual parameters between the Tyr47Phe and Tyr47Gly mutants were observed. While the Tyr47Phe mutation led to six times lower K_d for DHE with practically no changes in its biological activity, the Tyr47Gly mutation resulted in 30 times lower K_d for DHE with significant changes in its biological activity. The possible explanation is a structural change in helix C evoked by glycine, the amino acid with the lowest tendency to form a helical structure (Pace and Scholtz, 1998) and unable to stack with the side chains of Pro42 and Tyr33, in contrast to phenylalanine.

These facts, together with other results, imply that the conformational change in the ω-loop induced by sterol binding might not be crucial in determining an elicitin's activity. This statement could be further supported by the fact that even though the complexes β-cinnamomin–ergosterol and β-cryptogein–ergosterol have practically the same structure (with deviations of about 0.4 Å for the C_α atoms) (Rodrigues *et al.*, 2006) and binding properties, they differ significantly in the induction of early events in tobacco cells (Bourque *et al.*, 1998). So, it is obvious that the activity of elicitins is more dependent on the presence of specific residues than on the ω-loop structure; the most probable candidates being lysine residues in helices A and D of basic elicitins (Boissy *et al.*, 1996). This assumption is further supported by the observed correlation between necrotic index and p*I* (Pernollet *et al.*, 1993) and by a clear impact of the Lys13Val mutation in helix A on induction of a defence response in tobacco plants (Odonohue *et al.*, 1995; Pleskova *et al.*, 2011).

A possible model for the signal transduction mechanism would be similar to those proposed for the AVR9/Cf-9 interaction in tomato or the NIP1/Rrs1 interaction in barley (van't Slot *et al.*, 2007; Wulff *et al.*, 2009). In both

Table 4. Summary of obtained results for different cryptogein mutants

The biological efficiency of the mutants in DHE and NBD-PC transfer from Table 1 is compared with the specific binding to the high-affinity sites on the plasma membrane from Fig. 4; with ability to induce the synthesis of ROS and phytoalexin capsidiol from Fig. 2; as well as with the percentages of common spots between mutants and wt cryptogein obtained by image analysis of 2-D gels using PDQuest software (Bio-Rad, USA) and resistance induction against oomycete *P. parasitica* from Fig. 3.

Mutation	DHE transfer	NBD-PC transfer	Binding to PM	AOS synthesis	Capsidiol accumulation	% of common spots with WT	Resistance induction
Wild type	+++	+++	+++	+++	+++	100	+++
V84F	+	+++	+++	+++	++	65	+++
L41F	+++	++	+	+	–	31	+
L41F/V84F	+	+++	+	–	–	19	–

cases a similar hyperbolical binding curve was found with similar binding parameters to those of elicitins (Kooman-Gersmann *et al.*, 1998; van't Slot *et al.*, 2007). In addition, as for AVR9 and NIP1, an elicitor high-affinity binding site has been identified in different plant cultivars or species, but the effective response was observed only in the resistant genotype. The proposed model assumes interaction of elicitins with a high-affinity primary binding site with broad specificity that is present in various plants. Consequently, the interaction of specific lysine residues is needed for interaction with a putative third component of the target protein complex, which is finally responsible for transduction of the signal. This component could be a protein with a leucine-rich repeat, such as are encoded by many *R* genes and in many cases are responsible for effector-triggered immunity (Jones and Dangl, 2006). In this model, the primary binding of elicitins is not the crucial event determining plant resistance and susceptibility, and only the presence of specific residues in the elicitin molecule, together with a third interacting component, leads to an effective response.

Supplementary data

Supplementary data can be found at *JXB* online.

Supplementary data. Methods and effect of L80F/V84F mutation on cryptogein biological activity.

Supplementary Table S1. Details of MS analysis.

Supplementary Table S2. Sequences of the oligonucleotides used for mutagenesis of cryptogein and qPCR primer sequences.

Supplementary Table S3. Effect of L80F/V84F mutation on accumulation of transcripts for PR and other defence-related proteins.

Supplementary Fig. S1. Transfer of sterols and fatty acids catalysed by proteins and binding plots.

Supplementary Fig. S2. Two-dimensional gel electrophoresis proteome maps of intercellular fluid determined 48 h after application of cryptogein and its mutants.

Acknowledgements

Michel Ponchet is gratefully acknowledged for assistance with *Phytophthora* resistance methodology (INRA, Sophia-Antipolis, France). Financial support by the Ministry of Education, Youth and Sports of the Czech Republic (MSM0021622413, MSM0021622415), the Grant Agency of the Czech Republic (501/11/1003 and 203/09/P248), and by the European Regional Development Fund (CETOCOEN, CZ.1.05/2.1.00/01.0001), is gratefully acknowledged.

References

Avdulov NA, Chochina SV, Igbavboa U, Warden CS, Schroeder F, Wood WG. 1999. Lipid binding to sterol carrier protein-2 is inhibited by ethanol. *Biochimica et Biophysica Acta* **1437,** 37–45.

Blein JP, Coutos-Thévenot P, Marion D, Ponchet M. 2002. From elicitins to lipid-transfer proteins; a new insight in cell signalling involved in plant defence mechanisms. *Trends in Plant Science* **7,** 293–296.

Boissy G, de La Fortelle E, Kahn R, Huet JC, Bricogne G, Pernollet JC, Brunie S. 1996. Crystal structure of a fungal elicitor secreted by *Phytophthora cryptogea*, a member of a novel class of plant necrotic proteins. *Structure* **4,** 1429–1439.

Boissy G, O'Donohue M, Gaudemer O, Perez V, Pernollet J, Brunie S. 1999. The 2.1 angstrom structure of an elicitin-ergosterol complex: a recent addition to the Sterol Carrier Protein family. *Protein Science* **8,** 1191–1199.

Bourque S, Binet MN, Ponchet M, Pugin A, Lebrun-Garcia A. 1999. Characterization of the cryptogein binding sites on plant plasma membranes. *Journal of Biological Chemistry* **274,** 34699–34705.

Bourque S, Ponchet M, Binet MN, Ricci P, Pugin A, Lebrun-Garcia A. 1998. Comparison of binding properties and early biological effects of elicitins in tobacco cells. *Plant Physiology* **118,** 1317–1326.

Buhot N, Douliez JP, Jacquemard A, *et al*. 2001. A lipid transfer protein binds to a receptor involved in the control of plant defence responses. *FEBS Letters* **509,** 27–30.

Casaretto JA, Corcuera LJ. 1995. Plant proteinase inhibitors, a defensive response against insects. *Biological Research* **28,** 239–249.

Dobeš P, Kmuníček J, Mikeš V, Damborský J. 2004. Binding of fatty acids to β-cryptogein: quantitative structure–activity relationships and design of selective protein mutants. *Journal of Chemical Information and Modeling* **44,** 2126–2132.

Facchini PJ, Chappell J. 1992. Gene family for an elicitor-induced sesquiterpene cyclase in tobacco. *Proceedings of the National Academy of Sciences, USA* **89,** 11088–11092.

Flor HH. 1971. Current status of gene-for-gene concept. *Annual Review of Phytopathology* **9,** 275.

Galiana E, Bonnet P, Conrod S, Keller H, Panabieres F, Ponchet M, Poupet A, Ricci P. 1997. RNase activity prevents the growth of a fungal pathogen in tobacco leaves and increases upon induction of systemic acquired resistance with elicitin. *Plant Physiology* **115,** 1557–1567.

Garcia-Brugger A, Lamotte O, Vandelle E, Bourque S, Lecourieux D, Poinssot B, Wendehenne D, Pugin A. 2006. Early signaling events induced by elicitors of plant defenses. *Molecular Plant–Microbe Interactions* **19,** 711–724.

Gincel E, Simorre JP, Caille A, Marion D, Ptak M, Vovelle F. 1994. 3-Dimensional structure in solution of a wheat lipid-transfer protein from multidimensional H-1-NMR data: a new folding for lipid carriers. *European Journal of Biochemistry* **226,** 413–422.

Gooley PR, Keniry MA, Dimitrov RA, Marsh DE, Keizer DW, Gayler KR, Grant BR. 1998. The NMR solution structure and characterization of pH dependent chemical shifts of the β-elicitin, cryptogein. *Journal of Biomolecular NMR* **12,** 523–534.

Grover A, Gowthaman R. 2003. Strategies for development of fungus-resistant transgenic plants. *Current Science* **84,** 330–340.

Guex N, Peitsch MC. 1997. SWISS-MODEL and the Swiss-PdbViewer: an environment for comparative protein modeling. *Electrophoresis* **18,** 2714–2723.

Hermanson GT. 1996. *Bioconjugate techniques*. San Diego, London: Academic Press.

Hiraga S, Ito H, Sasaki K, Yamakawa H, Mitsuhara I, Toshima H, Matsui H, Honma M, Ohashi Y. 2000. Wound-induced expression of a tobacco peroxidase is not enhanced by ethephon and suppressed by methyl jasmonate and coronatine. *Plant and Cell Physiology* **41,** 165–170.

Hirasawa K, Amano T, Shioi Y. 2004. Lipid-binding form is a key conformation to induce a programmed cell death initiated in tobacco BY-2 cells by a proteinaceous elicitor of cryptogein. *Physiologia Plantarum* **121,** 196–203.

Hugot K, Aime S, Conrod S, Poupet A, Galiana E. 1999. Developmental regulated mechanisms affect the ability of a fungal pathogen to infect and colonize tobacco leaves. *The Plant Journal* **20,** 163–170.

Jones JDG, Dangl JL. 2006. The plant immune system. *Nature* **444,** 323–329.

Keller H, Bonnet P, Galiana E, Pruvot L, Friedrich L, Ryals J, Ricci P. 1996. Salicylic acid mediates elicitin-induced systemic acquired resistance, but not necrosis in tobacco. *Molecular Plant–Microbe Interactions* **9,** 696–703.

Kooman-Gersmann M, Vogelsang R, Vossen P, van den Hooven HW, Mahe E, Honee G, de Wit PJGM. 1998. Correlation between binding affinity and necrosis-inducing activity of mutant AVR9 peptide elicitors. *Plant Physiology* **117,** 609–618.

Literakova P, Lochman J, Zdrahal Z, Prokop Z, Mikes V, Kasparovsky T. 2010. Determination of capsidiol in tobacco cells culture by HPLC. *Journal of Chromatographic Science* **48,** 436–440.

Lochman J, Kašparovský T, Damborský J, Osman H, Marais A, Chaloupková R, Ponchet M, Blein JP, Mikeš V. 2005. Construction of cryptogein mutants, a proteinaceous elicitor from *Phytophthora*, with altered abilities to induce a defense reaction in tobacco cells. *Biochemistry* **44,** 6565–6572.

Luderer R, Rivas S, Nurnberger T, *et al*. 2001. No evidence for binding between resistance gene product Cf-9 of tomato and avirulence gene product AVR9 of *Cladosporium fulvum*. *Molecular Plant–Microbe Interactions* **14,** 867–876.

Melchers LS, Apothekerdegroot M, Vanderknaap J, Ponstein AS, Selabuurlage MB, Bol JF, Cornelissen BJC, Vandenelzen PJM, Linthorst HJM. 1994. A new class of tobacco chitinases homologous to bacterial exo-chitinases displays antifungal activity. *The Plant Journal* **5,** 469–480.

Mikes V, Milat ML, Ponchet M, Ricci P, Blein JP. 1997. The fungal elicitor cryptogein is a sterol carrier protein. *FEBS Letters* **416,** 190–192.

Mikes V, Milat ML, Ponchet M, Panabieres F, Ricci P, Blein JP. 1998. Elicitins, proteinaceous elicitors of plant defense, are a new class of sterol carrier proteins. *Biochemical and Biophysical Research Communications* **245,** 133–139.

Nicot N, Hausman JF, Hoffmann L, Evers D. 2005. Housekeeping gene selection for real-time RT-PCR normalization in potato during biotic and abiotic stress. *Journal of Experimental Botany* **56,** 2907–2914.

Odonohue MJ, Gousseau H, Huet JC, Tepfer D, Pernollet JC. 1995. Chemical synthesis, expression and mutagenesis of a gene encoding beta-cryptogein, an elicitin produced by *Phytophthora cryptogea*. *Plant Molecular Biology* **27,** 577–586.

Okushima Y, Koizumi N, Kusano T, Sano H. 2000. Secreted proteins of tobacco cultured BY2 cells; identification of a new member of pathogenesis-related proteins. *Plant Molecular Biology* **42,** 479–488.

Osman H, Vauthrin S, Mikes V, Milat ML, Panabières F, Marais A, Brunie S, Maume B, Ponchet M, Blein JP. 2001. Mediation of elicitin activity on tobacco is assumed by elicitin-sterol complexes. *Molecular Biology of the Cell* **12,** 2825–2834.

Pace CN, Scholtz JM. 1998. A Helix Propensity Scale based on experimental studies of peptides and proteins. *Biophysical Journal* **75,** 422–427.

Pernollet JC, Sallantin M, Salletourne M, Huet JC. 1993. Elicitin isoforms from 7 *Phytophthora* species: comparison of their physicochemical properties and toxicity to tobacco and other plant-species. *Physiological and Molecular Plant Pathology* **42,** 53–67.

Pleskova V, Kasparovsky T, Oboril M, Ptackova N, Chaloupkova R, Ladislav D, Damborsky J, Lochman J. 2011. Elicitin-membrane interaction is driven by a positive charge on the protein surface: role of Lys13 residue in lipids loading and resistance induction. *Plant Physiology and Biochemistry* **49,** 321–328.

Poinssot B, Vandelle E, Bentejac M, Adrian M, Levis C, Brygoo Y, Garin J, Sicilia F, Coutos-Thevenot P, Pugin A. 2003. The endopolygalacturonase 1 from *Botrytis cinerea* activates grapevine defense reactions unrelated to its enzymatic activity. *Molecular Plant–Microbe Interactions* **16,** 553–564.

Ponchet M, Panabieres F, Milat ML, Mikes V, Montillet JL, Suty L, Triantaphylides C, Tirilly Y, Blein JP. 1999. Are elicitins cryptograms in plant–oomycete communications? *Cellular and Molecular Life Sciences* **56,** 1020–1047.

Ricci P, Bonnet P, Huet JC, Sallantin M, Beauvaiscante F, Bruneteau M, Billard V, Michel G, Pernollet JC. 1989. Structure and activity of proteins from pathogenic fungi: *Phytophthora*-eliciting necrosis and acquired-resistance in tobacco. *European Journal of Biochemistry* **183,** 555–563.

Rodrigues ML, Archer M, Martel P, *et al*. 2006. Crystal structures of the free and sterol-bound forms of beta-cinnamomin. *Biochimica et Biophysica Acta-Proteins and Proteomics* **1764,** 110–121.

Rohini VK, Rao KS. 2001. Transformation of peanut (*Arachis hypogaea* L.) with tobacco chitinase gene, variable response of transformants to leaf spot disease. *Plant Science* **160,** 889–898.

Selabuurlage MB, Ponstein AS, Bresvloemans SA, Melchers LS, Vandenelzen PJM, Cornelissen BJC. 1993. Only specific tobacco (*Nicotiana tabacum*) chitinases and beta-1,3-glucanases exhibit antifungal activity. *Plant Physiology* **101,** 857–863.

Shinya T, Hanai K, Galis I, Suzuki K, Matsuoka K, Matsuoka H, Saito M. 2007. Characterization of NtChitIV, a class IV chitinase induced by beta-1,3-, 1,6-glucan elicitor from *Alternaria alternata* 102. Antagonistic effect of salicylic acid and methyl jasmonate on the

induction of NtChitIV. *Biochemical and Biophysical Research Communications* **353,** 311–317.

Sun JY, Gaudet DA, Lu ZX, Frick M, Puchalski B, Laroche A. 2008. Characterization and antifungal properties of wheat nonspecific lipid transfer proteins. *Molecular Plant–Microbe Interactions* **21,** 346–360.

Svozilová Z, Kašparovský T, Skládal P, Lochman J. 2009. Interaction of cryptogein with its binding sites in tobacco plasma membrane studied using the piezoelectric biosensor. *Analytical Biochemistry* **390,** 115–120.

van't Slot KAE, Gierlich A, Knogge W. 2007. A single binding site mediates resistance- and disease-associated activities of the effector protein NIP1 from the barley pathogen *Rhynchosporium secalis*. *Plant Physiology* **144,** 1654–1666.

van Loon LC, Rep M, Pieterse CM. 2006. Significance of inducible defense-related proteins in infected plants. *Annual Review of Phytopathology* **44,** 135–162.

Vauthrin S, Mikes V, Milat ML, Ponchet M, Maume B, Osman H, Blein JP. 1999. Elicitins trap and transfer sterols from micelles, liposomes and plant plasma membranes. *Biochimica et Biophysica Acta* **1419,** 335–342.

Wendehenne D, Binet MN, Blein JP, Ricci P, Pugin A. 1995. evidence for specific, high-affinity binding-sites for a proteinaceous elicitor in tobacco plasma-membrane. *FEBS Letters* **374,** 203–207.

Wong JH, Ng TB, Cheung RCF, *et al*. 2010. Proteins with antifungal properties and other medicinal applications from plants and mushrooms. *Applied Microbiology and Biotechnology* **87,** 1221–1235.

Wood MJ, Komives EA. 1999. Production of large quantities of isotopically labeled protein in Pichia pastoris by fermentation. *Journal of Biomolecular NMR* **13,** 149–159.

Wulff BBH, Chakrabarti A, Jones DA. 2009. Recognitional specificity and evolution in the tomato–*Cladosporium fulvum* pathosystem. *Molecular Plant–Microbe Interactions* **22,** 1191–1202.